Rapid Reduction of Nitric Oxide to Dinitrogen by Zirconium(II): Kinetic Studies on a Reaction Controlled by Gas−Liquid Transport

Kristopher McNeill*,† and Robert G. Bergman

Contribution from the Department of Chemistry, University of California, Berkeley, California 94720

Received August 21, 1998

Abstract: Nitric oxide reacts with $Cp_2Zr(PMe_3)_2$ (**1**; Cp = η^5-C_5H_5) in THF or toluene to yield dinitrogen and an oligomeric oxozirconocene species, $[Cp_xZrO_y]_n$. The reduction of NO occurs in two distinct steps: **1** reduces 2 equiv of NO to 1 equiv of N_2O, and then **1** reduces N_2O to N_2. In each step, **1** is converted to a monomeric oxozirconocene species [Cp_2ZrO], which may be trapped by the addition of Me_3SiCl or Cp_2ZrMe_2, to form $Cp_2Zr(OSiMe_3)(Cl)$ and $[Cp_2ZrMe]_2O$, respectively. Kinetics for the reduction of NO by **1** were followed at low temperature ($160 < T < 195$ K) by monitoring the change in pressure of the system. Complete reaction was observed in less than 15 s, even at the lowest temperatures. The typical kinetic trace displayed two decay regimes, zero- and first-order, which were interpreted as the result of competing mass-transfer and chemical reaction processes. The kinetic results support a rate-limiting bimolecular reaction between NO and **1**. The subsequent intermediates and mechanistic possibilities are discussed.

Introduction

The interconversion of nitrogen oxide species is important in biological[1−4] and environmental[5] processes. Transition metals play a prominent role in nitrogen reduction and oxidation in biotic nitrogen cycling (by metalloenzymes[6]) and in conversion of anthropogenic nitrogen oxide species to N_2.[7,8] The reaction of nitrogen oxides with well-characterized organometallic complexes might provide good models for these systems, but little is known about the mechanisms of such reactions, especially those that involve direct interactions with paramagnetic NO.[9−14] We report here that the Zr(II) complex $Cp_2Zr(PMe_3)_2$ reacts exceedingly rapidly with NO, even at −113 °C, ultimately leading to N_2 (eq 1) through the intermediacy of N_2O, and we give preliminary information on the mechanism of both steps in this transformation.

$$2\ NO \xrightarrow{Cp_2Zr(PMe_3)_2} N_2O \xrightarrow{Cp_2Zr(PMe_3)_2} N_2 \qquad (1)$$

Results

Reactions of $Cp_2Zr(PMe_3)_2$ with NO and N_2O. When solutions of $Cp_2Zr(PMe_3)_2$ (**1**) are treated with gaseous NO at room temperature (or below), bleaching of the characteristic black-red color is observed, and a colorless precipitate is produced. The gaseous N-containing products are N_2O and N_2, identified by FTIR (N_2O) and GC (N_2O and N_2). The organometallic products are less well-defined. The only product observable by ^{1}H NMR spectroscopy is the previously reported[15] oxo trimer, $[Cp_2ZrO]_3$, which typically accounts for 21% of the Zr-containing species. The remainder of the Zr-containing material is presumed to be an insoluble oligomeric zirconium oxo complex, $[Cp_xZrO_y]_n$, thought to arise (see evidence summarized below) by oligomerization of monomeric $Cp_2Zr{=}O$.[15] The absence of nitrogen in the insoluble precipitate is confirmed by combustion analysis. The insoluble material may be a polymer (e.g., $[Cp_2ZrO]_n$), a cluster (e.g., $Cp_4Zr_4O_6$, by analogy to the material formed when $(C_5Me_5)_2M(C_2H_4)$ (M = Ti, V) are exposed to N_2O[16]), or a mixture of the two.

When the reaction of **1** and NO is carried out with a strictly stoichiometric amount (2 equiv) of nitric oxide, N_2O is observed as the reduced N-containing product. With a molar deficiency of NO, N_2 is observed as the predominant N-containing product. This indicates that two sequential O-atom-transfer steps are involved in the complete reduction of NO to N_2. The first involves reaction of 2 equiv of NO with **1** to produce $Cp_2Zr{=}O$ and N_2O (eq 2), and the second is the reaction of N_2O with **1** (eq 3), leading to N_2 and a second equivalent of $Cp_2Zr{=}O$.

$$1 + 2\ NO \longrightarrow N_2O + [Cp_2ZrO] \qquad (2)$$

$$1 + N_2O \longrightarrow N_2 + [Cp_2ZrO] \qquad (3)$$

The second stage in this process can be observed directly. When solutions of $Cp_2Zr(PMe_3)_2$ (**1**) are exposed to N_2O at −78 °C, fast reaction occurs with deposition of $[Cp_xZrO_y]_n$. As with

† Current address: Department of Chemistry, University of Minnesota, 207 Pleasant St. SE, Minneapolis, MN 55455.

(1) Delwiche, C. C. *Denitrification, Nitrification and Atmospheric Nitrous Oxide*; John Wiley and Sons: New York, 1981.
(2) Smil, V. *Carbon Nitrogen Sulfur: Human Interference in Grand Biospheric Cycles*; Plenum Press: New York, 1985.
(3) Butler, A. R.; Williams, D. L. H. *Chem. Soc. Rev.* **1993**, 233.
(4) Payne, W. J. *Denitrification*; John Wiley and Sons: New York, 1981.
(5) Schwartz, S. E.; White, W. H. In *Trace Atmospheric Constituents: Properties, Transformation and Fates*; Schwartz, S. E., Ed.; John Wiley and Sons: New York, 1983; Vol. 12.
(6) Kroneck, P. M. H.; Beuerle, J.; Schumacher, W. In *Degradation of Environmental Pollutants by Microorganisms and their Metalloenzymes*; Sigel, H., Sigel, A., Eds.; Marcel Dekker: New York, 1992; Vol. 28.
(7) Armor, J. N. *Environmental Catalysis*; American Chemical Society: Washington, DC, 1994.
(8) Armor, J. N. *Appl. Catal. B* **1992**, *1*, 221.
(9) MacNeil, J. H.; Berseth, P. A.; Westwood, G.; Trogler, W. C. *Environ. Sci. Technol.* **1998**, *32*, 876.
(10) MacNeil, J. H.; Berseth, P. A.; Bruner, E. L.; Perkins, T. L.; Wadia, Y.; Westwood, G.; Trogler, W. C. *J. Am. Chem. Soc.* **1997**, *119*, 1668.
(11) MacNeil, J. H.; Gantzel, P. K.; Trogler, W. C. *Inorg. Chim. Acta* **1995**, *240*, 299.
(12) Meyer, C. D.; Eisenberg, R. *J. Am. Chem. Soc.* **1976**, *98*, 1364.
(13) Hendriksen, D. E.; Meyer, C. D.; Eisenberg, R. *Inorg. Chem.* **1977**, *16*, 970.
(14) Haymore, B. L.; Ibers, J. A. *J. Am. Chem. Soc.* **1974**, *96*, 3325.

10.1021/ja983011p CCC: $18.00
Published on Web 08/31/1999

Scheme 1

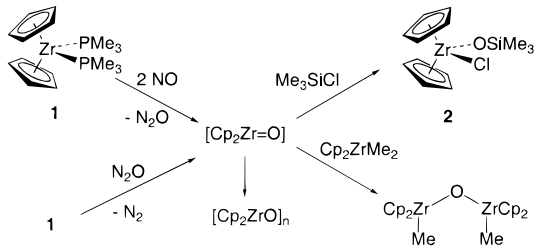

the reaction of **1** and NO, the only soluble Zr-containing product seen by NMR spectroscopy is $[Cp_2ZrO]_3$, and this accounts for 26% of the Zr-containing species by integration vs an internal standard. Analysis of the gas phase by GC shows consumption of N_2O and production of N_2 in 86% conversion.

Evidence for $Cp_2Zr{=}O$ as a Product: Trapping Experiments. Evidence for the initial formation of monomeric $Cp_2Zr{=}O$ as the first-formed product in this reaction was obtained by chemical trapping studies. Carrying out the reaction of **1** with NO in the presence of 2 equiv of Me_3SiCl eliminated the formation of precipitate and gave, instead, $Cp_2Zr(OSiMe_3)(Cl)$[17] (**2**, 77% conversion based on ^1H NMR integration vs an internal standard, Scheme 1).

Similarly, treatment of **1** with N_2O in the presence of Me_3SiCl also gave complex **2** (100% conversion). Employing Cp_2ZrMe_2 as a trap, suggested earlier to be an efficient trap for $Cp_2Zr{=}O$,[18,19] gave $[Cp_2ZrMe]_2O$ from the reaction of **1** and N_2O in 76% yield by NMR (Scheme 1).

We considered the possibility that the products from these experiments did not arise from trapping of the intermediate but instead from reaction of the added trap with the oligomeric species. However, control experiments showed that allowing the reaction of **1** with NO or N_2O to proceed to give oligomeric $[Cp_xZrO_y]_n$, followed by addition of Me_3SiCl, does not give **2** (eq 4). This reinforces the conclusion that a reactive precursor

$$[Cp_2ZrO]_3 + [Cp_xZrO_y]_n + Me_3SiCl \not\longrightarrow \mathbf{2} \qquad (4)$$

to $[Cp_xZrO_y]_n$, presumably a monomeric oxo species,[18] is being trapped by Me_3SiCl and that oligomerization of this species is irreversible under these conditions.

Role of PMe_3 in the Reduction of NO. One potential complication in the analysis of this system is that free PMe_3 is also known to undergo rapid oxidation by NO, forming N_2O and $Me_3P{=}O$.[20] No $Me_3P{=}O$ was detected when the reaction of **1** was carried out with a molar deficiency of NO, as indicated by ^1H NMR spectroscopic analysis. However, $Me_3P{=}O$ could be produced and then rapidly consumed by **1** (Scheme 2, path b).

To rule out this possibility, **1** was treated with $Me_3P{=}O$ in C_6D_6 at 20 °C. No reaction was observed under these conditions, demonstrating that the reaction of PMe_3 with NO is slower than the reaction of **1** with NO (see also Kinetic Studies). Thus, if $Me_3P{=}O$ were formed during the reaction of **1** with NO, it would persist and be detected. Given these facts, it is clear that,

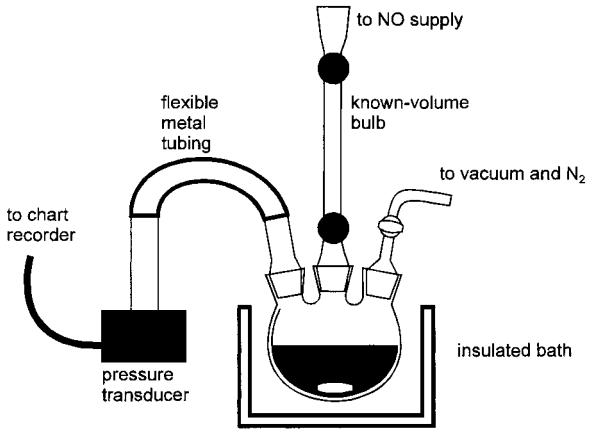

Figure 1. Schematic representation of the experimental apparatus used for measuring the kinetics of NO reduction by the change in pressure.

Scheme 2

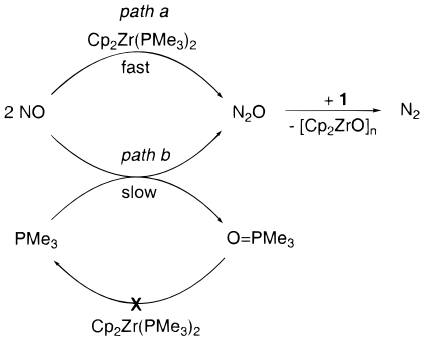

when NO is present in a limiting amount, the species that is active in converting $2NO \rightarrow N_2O \rightarrow N_2$ is **1** and not PMe_3 (Scheme 2, path a).

Even though **1** reacts with NO much more quickly than does PMe_3, the presence of the phosphine causes the N_2/N_2O ratios produced in the reaction of **1** with NO to vary greatly, depending on the conditions. It is simplest to consider two limiting cases. When 1 equiv or less of NO is treated with complex **1**, all of the NO will be converted to N_2O, and all of the N_2O produced will be consumed to give N_2 (eq 5). In the other extreme, when

$$Cp_2Zr(PMe_3)_2 + 1\ NO \longrightarrow [Cp_2ZrO] + 2\ PMe_3 + {}^1/_2\ N_2 \qquad (5)$$

complex **1** is exposed to a large excess of NO, such that all of **1** is consumed by NO in the first step and no amount of **1** is left to react with N_2O, it is expected that only N_2O will be produced. In this latter case, up to 6 equiv of NO will be consumed, since the metal complex can react with 2 equiv and the two phosphine ligands will each react with 2 equiv of NO after **1** has been consumed (eq 6). These two extremes have

$$Cp_2Zr(PMe_3)_2 + 6\ NO \longrightarrow [Cp_2ZrO] + 2\ OPMe_3 + 3\ N_2O \qquad (6)$$

been approximated experimentally. With NO as the limiting reagent, we have found by gas chromatographic analysis that NO is converted to N_2 in 86% yield. With excess NO, FTIR analysis indicates that conversion to N_2O is 69−87% based on the stoichiometry of eq 6.

Kinetic Studies. It was possible to measure the rate of NO consumption by the pressure change associated with the conversion of 2NO to $1N_2O$. The reactions were performed in a three-necked flask fitted with a known-volume bulb and a pressure transducer (Figure 1). The reaction flask contained a rapidly stirred solution of either PMe_3 or **1** in THF and was

(15) Fachinetti, G.; Floriani, C.; Chiesi-Villa, A.; Guastini, C. *J. Am. Chem. Soc.* **1979**, *101*, 1767.
(16) Smith, M. R., III; Matsunaga, P. T.; Andersen, R. A. *J. Am. Chem. Soc.* **1993**, *115*, 7049.
(17) Tilley, T. D. *Organometallics* **1985**, *4*, 1452.
(18) Lee, S. Y.; Bergman, R. G. *J. Am. Chem. Soc.* **1996**, *118*, 6396.
(19) Hanna, T. A.; Baranger, A. M.; Walsh, P. J.; Bergman, R. G. *J. Am. Chem. Soc.* **1995**, *117*, 3292.
(20) Halmann, M.; Kugel, L. *J. Chem. Soc.* **1962**, 3272.

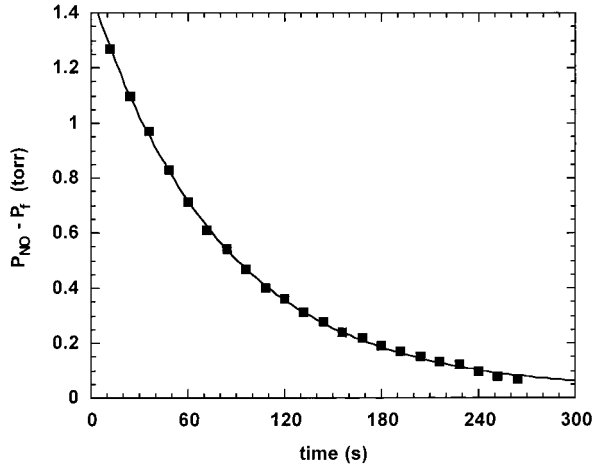

Figure 2. Typical kinetic trace for the reaction of PMe_3 and NO (entry 3, Table 3). The solid line corresponds to a best-fit exponential function with a decay constant, $k_{obs} = 0.0122 \pm 0.0002$ s^{-1}, and $r^2 = 0.9995$.

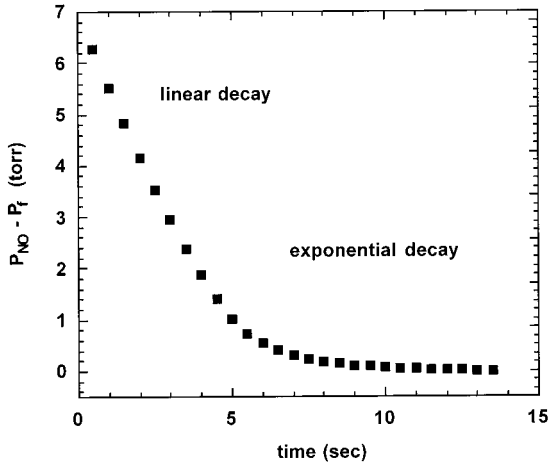

Figure 3. Typical kinetic trace for the reaction of **1** and NO (entry 6, Table 5). The best-fit line by least-squares regression for data for which $0 \le t \le 3$ s has a slope of $m = -16.1 \pm 0.03$ μmol s^{-1} and $r^2 = 0.9983$. This slope corresponds to a value for the NO flux $J_{NO} = 1.71 \pm 0.04$ μmol cm^{-2} s^{-1}. The best-fit exponential decay for the data collected after 4 s has a decay constant of $k_{obs} = 0.617 \pm 0.008$ s^{-1} and $r^2 = 0.9994$.

evacuated prior to introduction of nitric oxide. A kinetic run was initiated by opening the stopcock separating the reaction flask and the bulb, which was precharged with NO. The pressure was observed to increase sharply and then decrease as the NO was consumed. This technique proved to be very convenient for the measurement of both slow rates ($t_{1/2} \approx 30$ min) and very fast rates ($t_{1/2} \approx 1$ s). The temperature could be controlled over a wide range, although lower temperatures, where the solvent vapor pressure was low, provided the best signal-to-noise ratios. Others have employed similar methods to measure the NO consumption rates with $P(OEt)_3$[21] and Rh salts.[22]

In this study, the reaction rates for the reduction of NO by both PMe_3 and **1** were measured. The study of the kinetics of the reaction of NO with PMe_3 was useful both for confirming its slower reaction rate (compared with that of **1**) and for providing a well-behaved system for comparison with the more complicated kinetics for NO with **1**.

The reaction of PMe_3 with NO (eq 7) was followed at −78 °C and was found to follow pseudo-first-order kinetics for the consumption of NO (Figure 2). This system was assumed to obey the second-order rate law established for the reaction of $P(OEt)_3$ and NO (eq 8).[21] Employing the method of Kuhn et

$$PMe_3 + 2\ NO \longrightarrow O{=}PMe_3 + N_2O \tag{7}$$

$$\left(\frac{d[PMe_3]}{dt}\right) = 1/2\left(\frac{dP_{NO}}{dt}\right) = -k[PMe_3]P_{NO} \tag{8}$$

al., a bimolecular rate constant for the consumption of NO by PMe_3 was calculated to be $(1.3 \pm 0.3) \times 10^{-2}$ M^{-1} s^{-1}.[21] When the rates of the reaction of **1** and NO were measured, the results differed from those measured for the reaction of PMe_3 with NO in two important ways. The reaction with **1** was observed to be much faster, and the kinetic traces were not simple first-order decays. Instead, the traces were characterized as having an initial zero-order (linear) decay, followed by a first-order (exponential) decay (Figure 3).

Both the zero-order and the first-order decreases in P_{NO} were found to be independent of [PMe_3]. While the zero-order rates varied directly with [**1**], the first-order rates did not. Instead, the first-order decay constants appear to scale with the square root of the metal concentration (see Discussion section). The role of the solvent, THF, was tested by performing the reactions in the less-coordinating, sterically hindered analogue,[23] 2,5-dimethyltetrahydrofuran (2,5-Me_2THF). The rates for both regimes were found to be the same within error for experiments performed in THF and 2,5-Me_2THF. The experimentally determined rate laws for the two regimes are given in eqs 9 and 10.

$$\left(\frac{d[\mathbf{1}]}{dt}\right) = 1/2\left(\frac{dP_{NO}}{dt}\right) = -k[\mathbf{1}] \qquad \text{high } P_{NO} \tag{9}$$

$$\left(\frac{d[\mathbf{1}]}{dt}\right) = 1/2\left(\frac{dP_{NO}}{dt}\right) = -k[\mathbf{1}]^{0.5}P_{NO} \quad \text{low } P_{NO} \tag{10}$$

The stirring rate affected the NO consumption rate differently for the two systems studied, showing a pronounced effect on the reaction of NO with **1** and a negligible one in the reaction of NO with PMe_3. The effects can be compared by plotting the relative rate constants (k_{rel}) vs stirring rate, normalizing the lowest stirring value to $k_{rel} = 1.0$ (Figure 4).

Discussion

General Observations. Oxygen-atom-transfer reactions involving Group 4 metallocene species have been of considerable interest.[16,24−32] Nitrous oxide (N_2O) has proven to be a relatively mild O-atom-transfer reagent for divalent Ti,[16,25−28,33] Zr,[29−31,34,35]

(21) Kuhn, L. P.; Doali, J. O.; Wellman, C. *J. Am. Chem. Soc.* **1960**, *82*, 4792.
(22) Reed, J.; Eisenberg, R. *Science* **1974**, *184*, 658.
(23) Wax, M. J.; Bergman, R. G. *J. Am. Chem. Soc.* **1981**, *103*, 7028.
(24) Vaughan, G. A.; Rupert, P. B.; Hillhouse, G. L. *J. Am. Chem. Soc.* **1987**, *109*, 5538.
(25) Polse, J. L.; Andersen, R. A.; Bergman, R. G. *J. Am. Chem. Soc.* **1995**, *117*, 5393.
(26) Bottomley, F.; Lin, I. J. B.; Mukaida, M. *J. Am. Chem. Soc.* **1980**, *102*, 5238.
(27) Bottomley, F.; Brintzinger, H. H. *J. Chem. Soc., Chem. Commun.* **1978**, 234.
(28) Vaughan, G. A.; Sofield, C. D.; Hillhouse, G. L.; Rheingold, A. L. *J. Am. Chem. Soc.* **1989**, *111*, 5491.
(29) Howard, W. A.; Trnka, T. M.; Waters, M.; Parkin, G. *J. Organomet. Chem.* **1997**, *528*, 95.
(30) Howard, W. A.; Parkin, G. *J. Am. Chem. Soc.* **1994**, *116*, 606.
(31) Howard, W. A.; Waters, M.; Parkin, G. *J. Am. Chem. Soc.* **1993**, *115*, 4917.
(32) Howard, W. A.; Parkin, G. *J. Organomet. Chem.* **1994**, *472*, C1.
(33) For a rare example in which N_2O reacts with a transition metal species without loss of N_2, see ref 28.

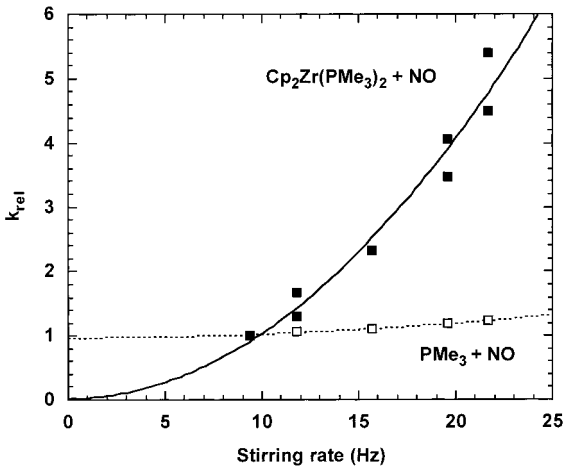

Figure 4. Effect of stirring rate on the observed reaction rate for PMe_3 + NO (■) and **1** + NO. (□) Pseudo-first-order rate constants for PMe_3 + NO normalized to $k_{rel} = 1$ for the lowest stirring rate. Initial zero-order fluxes (J_{NO}) for **1** + NO normalized to $k_{rel} = 1$ for the lowest stirring rate. The lines are parabolic fits to the data ($y = a + bx^2$).

and Hf [32,36,37] metallocene complexes. Terminal and bridging oxo species as well as oxygen-insertion products are known to be formed in these reactions. In contrast, the interaction of nitric oxide (NO) with Group 4 metallocenes is poorly understood. Well-defined Group 4 nitrosyl complexes appear to be extremely rare.[38] Bottomley and co-workers have examined reactions of $Cp_2Ti(CO)_2$ with NO and have found that oxidized Ti-containing species and reduced N-containing species are formed.[27,39] However, these transformations are relatively complicated. Depending on stoichiometry, temperature, solvent, and other factors, the products may include N_2O, N_2, isocyanate complexes, hyponitrite complexes, and titanium oxo species.[27,39]

By comparison, the overall reaction of $Cp_2Zr(PMe_3)_2$ with NO is apparently uncomplicated. Nitric oxide is completely reduced by **1** to dinitrogen, and the experimental results indicate that this transformation occurs in two distinct steps: the reduction of 2NO to N_2O, followed by reduction of N_2O to N_2. Both of these steps are very fast, even at reduced temperatures. The reaction of NO and **1** is complete within 15 s at −113 °C (from kinetic studies), and the reaction of N_2O and **1** is complete within minutes at −80 °C (low-temperature NMR studies) and may be considerably faster.[40]

Despite the rapidity of these transformations, a fair amount of mechanistic information regarding them has been obtained. In both the reduction of NO and N_2O, a transient oxozirconium species is formed which may be trapped. The trapping of monomeric Group 4 oxo species has been developed only in the past decade, and the set of efficient oxo traps fit broadly into two classes: those that keep the M═O bond intact and those that react with it. No traps of the former class (e.g., pyridines, phosphine oxides, amines, ethers) have been found that efficiently trap Cp_2Zr═O and prevent oligomerization, either earlier[18,19] or in this study. The successful traps employed in this study were of the latter class. Cp_2ZrMe_2 and Me_3SiCl proved to be efficient traps, providing the bridging oxo species $(Cp_2ZrMe)_2O$ and $Cp_2Zr(OSiMe_3)(Cl)$, respectively.[41] Other known traps for Cp_2Zr═O were found to react either with **1** or with the nitrogen oxide reagent.

Scheme 3

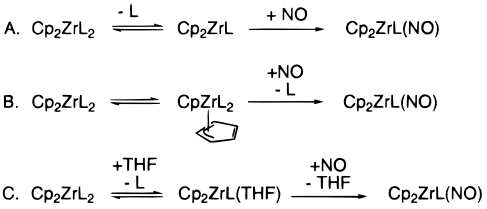

Kinetic Studies. Two-regime kinetic traces, like those obtained for the reaction of **1** with NO, are characteristic of systems exhibiting saturation behavior. A general mechanistic scheme that would predict such behavior is one involving a reversible first step, followed by an irreversible second step. Sensible mechanisms can be written that employ either only chemical transformations or both chemical and mass-transfer steps. Two mechanistic hypotheses involving only chemical reactions which seem particularly reasonable are those involving either initial reversible phosphine dissociation (Scheme 3A) or initial reversible Cp slippage (change in binding mode from η^5 to η^3) (Scheme 3B). Both of these hypothetical mechanisms involve opening a coordination site at the metal center for NO binding and represent dissociative and associative ligand substitution schemes consistent with saturation kinetics. In addition to these, a mechanism which involves reversible attack of the solvent on the complex, followed by irreversible reaction with NO, would also predict saturation kinetics (Scheme 3C).

Several pieces of data argue against these three possible mechanisms. The very small effect of temperature on the rate is inconsistent with the enthalpy of activation expected for an initial bond cleavage (either Zr−PMe_3 or Zr−Cp). The lack of any effect on the kinetic traces due to added PMe_3 (0−1 M) rules out a reversible phosphine dissociation mechanism. The fact that no change in rate is observed when the solvent is changed from THF to 2,5-Me_2THF argues against the participation of a solvent molecule. Most importantly, none of these mechanisms can account for the pronounced effect of stirring speed on the rate of NO consumption.

The effect of stirring speed indicates that the reaction of **1** with NO is controlled, to a large degree, by the rate of mass transfer of NO into solution. Comparing the observed NO absorption rates vs stirring speed for the reaction of **1** with NO and PMe_3 with NO gives the clearest picture of how stirring affects the rate (Figure 4). For the reaction of **1** with NO, the rate dramatically changes with different stirring speeds, a clear indication that the mass-transfer rate is important to the observed rate of reaction. Indeed, an empirical correlation of the NO absorption rate and the square of the stirring rate is observed. By comparison, the rate change for the reaction of PMe_3 with NO is negligible for different stirring rates, demonstrating that mass transfer is a much less important part of the overall rate of NO consumption for this inherently slower reaction.

There are many studies of the uptake of a gas by a solution containing a chemically reactive species.[42−44] Astarita has

(34) Vaughan, G. A.; Hillhouse, G. L.; Rheingold, A. L. *J. Am. Chem. Soc.* **1990**, *112*, 7994.

(35) Vaughan, G. A.; Hillhouse, G. L.; Lum, R. T.; Buchwald, S. L.; Rheingold, A. L. *J. Am. Chem. Soc.* **1988**, *110*, 7215.

(36) The reaction of $Cp^*_2Hf(Ph)(H)$ with N_2O (ref 24) is proposed to proceed through the benzyne complex (refs 34 and 35).

(37) In contrast to the reaction of $Cp^*_2Zr(CO)_2$ with N_2O (refs 29−31), $Cp^*_2Hf(CO)_2$ and N_2O are reported not react to give well-defined products (ref 32).

(38) Richter-Addo, G. B.; Legzdins, P. *Metal Nitrosyls*; Oxford University Press: New York, 1992.

(39) Bottomley, F.; Lin, I. J. B. *J. Chem. Soc., Dalton Trans.* **1981**, 271.

(40) Notable is the extreme difference in the reaction conditions required to initiate reaction between N_2O and **1** (−78 °C, <10 m) and N_2O and $Cp_2Zr(CO)_2$ (+80 °C, 12 h, ref 29).

(41) Me_3SiCl is known to react with Cp^*_2Zr═O to form $Cp^*_2Zr(OSiMe_3)(Cl)$, or $Cp^*_2ZrCl_2$ and $(Me_3Si)_2O$ (ref 29).

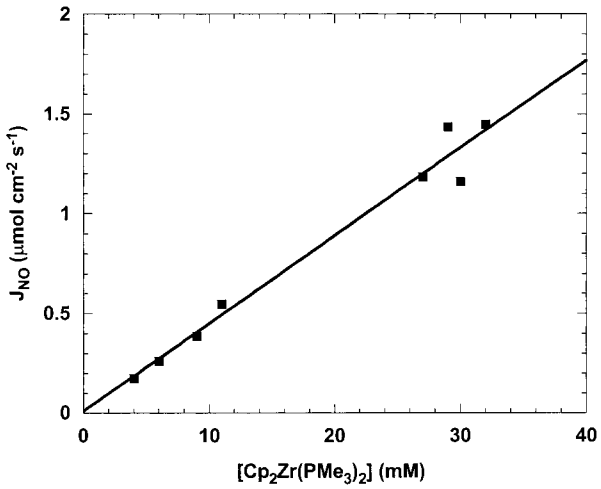

Figure 5. Zero-order flux (μmol cm^{-2} s^{-1}) at 195 K vs [**1**] (mM), showing a linear dependence. The best-fit line by least-squares regression has slope $m = 0.044 \pm 0.003$ cm s^{-1}, intercept $b = 0.01 \pm 0.07$ μmol cm^{-2} s^{-1}, and $r^2 = 0.9724$.

summarized the results of these studies and identified four important regimes: slow reaction−diffusional, slow reaction−kinetic, fast reaction, and instantaneous reaction regimes.[44] The flux of the gas into solution for each of these scenarios is well understood, and the four regimes can be distinguished by a number of tests. Using the criteria outlined by Astarita,[44] we suggest that the uptake of NO by a solution of **1** is a process at the boundary of the fast reaction and instantaneous reaction regimes. At low NO pressures, the uptake is in the fast reaction regime, and at higher NO pressures it is in the instantaneous reaction regime.

The zero-order consumption of NO by solutions of **1** at high NO pressures ($P_{NO} > 1$ Torr) is a clear indication that the absorption process is in the instantaneous reaction regime. For all other chemical absorption regimes, there is some dependence of the flux on the interfacial gas concentration.[44] To be in this regime, the rate of chemical reaction does not need to be "instantaneous", but rather it must be fast enough so that a small volume near the liquid surface becomes completely depleted in **1**. The result is that the uptake is controlled by the rate at which **1** can diffuse toward the surface to meet the incoming NO. The flux of NO, J_{NO}, entering the solution is given by eq 11, where k_L^o is the physical mass-transfer velocity of NO into solution (in cm/s) and D is the diffusivity of NO and **1** (in cm^2/s).[44] Because $[NO]_{interface} \ll [\mathbf{1}]_{bulk}$, the flux can be approximated by eq 12. A linear relationship between the zero-order flux and

$$J_{NO} = k_L^o \left(\left(\frac{D_1}{D_{NO}} \right)^{2/3} [\mathbf{1}]_{bulk} + \left(\frac{D_{NO}}{D_1} \right)^{1/3} [NO]_{interface} \right) \quad (11)$$

$$J_{NO} = k_L^o \left(\frac{D_1}{D_{NO}} \right)^{2/3} [\mathbf{1}]_{bulk} \quad (12)$$

[**1**] can clearly be seen (Figure 5). From this plot, using a diffusivity ratio of $D_1/D_{NO} = 0.15$ (see Appendix), a transfer velocity, k_L^o, of 0.16 ± 0.01 cm/s is obtained.

Because [**1**] near the surface is completely depleted in the instantaneous reaction regime, the NO can have a small, but

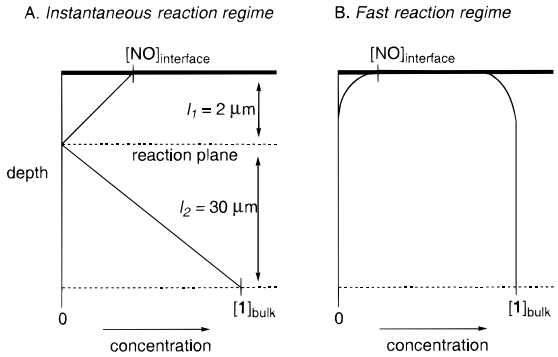

Figure 6. Schematic representations of the concentration gradients of NO and **1** near the gas−liquid interface (adapted from Astarita[44]). (A) In the instantaneous reaction regime, the reaction rate is limited by the diffusional transport of **1** from below. (B) In the fast reaction regime, the transport of **1** is no longer limiting. Instead, the rate of NO absorption is related to both the diffusivity of NO and the rate of chemical reaction. These figures are not drawn to scale.

significant, penetration depth into the solution. The surface-film concentration gradients are shown schematically in Figure 6A. The reaction plane, where NO and **1** meet, is at the depth determined by the relative diffusivities and concentrations of the two species. This can be shown by considering the fluxes of the two species. According to Fick's law, the flux of NO into solution is given by eq 13, where l_1 is the distance from the interface to the reaction plane. Similarly, the flux of **1** toward the surface is given by eq 14, where l_2 is the distance from the bottom of the surface film to the reaction plane. Since the two fluxes must be equal, one can combine these expressions to give eq 15. The result is that the ratio of the diffusion lengths can be determined from the diffusivities and the bulk and interface concentrations of the reacting species. The ratio of concentrations in this regime is typically on the order of 10^2, which results in a ratio of $l_2/l_1 \approx 15$.

$$J_{NO} = \frac{D_{NO}[NO]_{interface}}{l_1} \quad (13)$$

$$J_1 = \frac{D_1[\mathbf{1}]_{bulk}}{l_2} \quad (14)$$

$$\frac{l_2}{l_1} = \frac{D_1}{D_{NO}} \frac{[\mathbf{1}]_{bulk}}{[NO]_{interface}} \quad (15)$$

In the fast reaction regime, the diffusion of the reactive solution species is no longer limiting. By contrast to the instantaneous reaction regime, the fast reaction regime is characterized by having a flux of a gas into solution which is related to the interfacial concentration of the gas. The flux of a compound, X, is proportional to the interfacial concentration raised to the $(n + 1)/2$ power (eq 16), where n is the reaction order.[44] Consequently, the reaction order of the absorbing

$$J_X \propto [X]^{(n+1)/2} \quad (16)$$

species can be determined experimentally. For first- and second-order reaction orders in X, the absorption rates are proportional to $[X]^1$ and $[X]^{3/2}$, respectively.

The absorption of NO by solutions of **1** is observed to be first-order at low NO pressures, indicating that the reaction order in NO is 1. An expression for J_{NO} in the fast reaction regime, assuming a first-order reaction in $[NO]_{interface}$, is given in eq 17, where m is the reaction order in [**1**].[44] One can see that the uptake rate is controlled by both the diffusivity of NO and the

(42) Sherwood, T. K.; Pigford, R. L.; Wilke, C. R. *Mass Transfer*; McGraw-Hill: New York, 1975.
(43) Atkins, P. W. *Physical Chemistry*, 4th ed.; W. H. Freeman and Co.: New York, 1990.
(44) Astarita, G. *Mass Transfer with Chemical Reaction*; Elsevier: Amsterdam, 1967.

$$J_{NO} = (D_{NO}k_{rxn}[\mathbf{1}]^m)^{0.5}[NO]_{interface} \quad (17)$$

reaction rate constant. The flux can be related to the first-order rate (expressed as the change in the number of moles of NO with respect to time, $d(n_{NO})/dt$) by recognizing that flux is equal to the rate divided by the interfacial area A (eq 18). Setting the

$$J_{NO} = \left(\frac{d(n_{NO})}{dt}\right)\left(\frac{1}{A}\right) = \frac{k_{obs}n_{NO}}{A} \quad (18)$$

two flux expressions (eqs 17 and 18) equal, one obtains an expression that predicts a square-root dependence of the observed rate constant, k_{obs}, on $[\mathbf{1}]^m$ (eq 19). The constants V_g

$$k_{obs} = (D_{NO}k_{rxn}[\mathbf{1}]^m)^{0.5}\left(\frac{A}{V_gH}\right) \quad (19)$$

and H in eq 19 are the gas-phase volume and the dimensionless Henry's law constant for NO in THF, respectively. They arise from the sequential conversions of $[NO]_{interface}$ first into a gas-phase concentration, $[NO]_g$, and then into the number of moles of NO, n_{NO}. A plot of k_{obs} vs $[\mathbf{1}]^{0.5}$ is reasonably linear ($r^2 = 0.765$ for the linear regression), indicating that the reaction is first-order in [**1**] and yields a bimolecular rate constant of $(1.5 \pm 0.3) \times 10^8$ M^{-1} s^{-1} (Figure 7). The expressed uncertainty is the propagated uncertainty of the line fit and, therefore, only takes into account the scatter in the data. Because the constants in eq 19 can also contribute to the uncertainty, with the two largest contributors being the values for H and A (see Appendix), the true uncertainty is much higher. It can be said that the derived value for k_{rxn} is an upper limit since the value of A used is a lower limit and k_{rxn} is proportional to $1/A^2$.

The transition between the instantaneous and fast reaction regimes occurs when the equality given in eq 20 is satisfied.[44] Empirically, the changeover is observed when the ratio $[\mathbf{1}]_{bulk}/[NO]_{interface}$ is on the order of 10^3. Given $k_{rxn} = 1.5 \times 10^8$ M^{-1} s^{-1} and a typical concentration of $[\mathbf{1}] = 10^{-2}$ M, a time constant for reaction, τ_{rxn}, of 6.7×10^{-7} s is calculated. The value of the time constant for diffusion, τ_D, from eq 20 is, therefore, approximately 0.67 s. This quantity is useful in determining

$$\frac{[\mathbf{1}]_{bulk}}{[NO]_{interface}} \approx \left(\frac{\tau_D}{\tau_{rxn}}\right)^{0.5} \quad (20)$$

the thickness of the surface film using the Einstein−Smoluchowskii equation, $\tau_D \approx l^2/D$, where l is the length scale of molecular diffusion.[43,45] Using a value of $D_{NO} = 1.1 \times 10^{-5}$ cm^2 s^{-1}, $l \approx 30$ μm.

From the parameters derived from the instantaneous, fast, and changeover regimes, a physical picture of the rate-controlling processes and length scales involved develops. The reaction between NO and **1** occurs in a surface film with an approximate thickness of 30 μm. The rate of reaction is extremely fast, $k_{rxn} = 1.5 \times 10^8$ M^{-1} s^{-1}, approaching the diffusion-controlled limit (5.8×10^9 M^{-1} s^{-1}, see Appendix). When the NO pressure is high enough, the incoming gas rapidly depletes the concentration of **1** in the volume near to the surface. The major consequence of this is that the consumption of NO in this regime is controlled by the diffusion of **1** from the bulk solution through the surface film, and the rate is "saturated". From eq 15, the NO is calculated to have a penetration depth into solution of approximately 2 μm. As the NO pressure decreases, it eventually reaches a point at which the mass transfer of **1** is no longer limiting. Instead, the rate of NO consumption is proportional to the pressure in the gas phase, giving rise to first-order absorption kinetics.

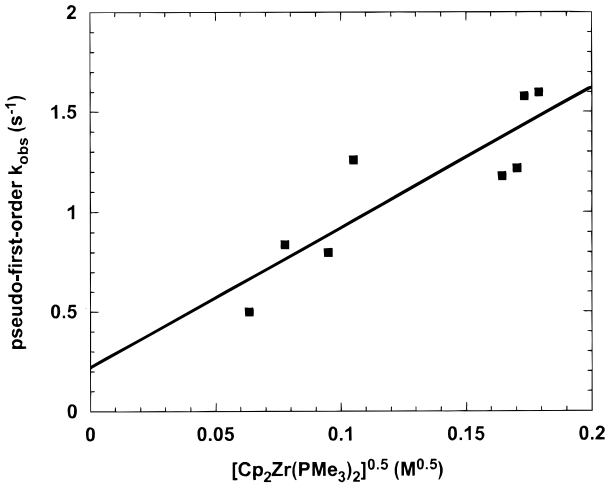

Figure 7. Pseudo-first-order rates (s^{-1}) at 195 K vs $[\mathbf{1}]^{0.5}$. The solid line corresponds to the least-squares best-fit line ($m = 7.0 \pm 1.6$ $M^{-0.5}$ s^{-1}, $b = 0.22 \pm 0.22$ s^{-1}, $r^2 = 0.7653$).

Scheme 4

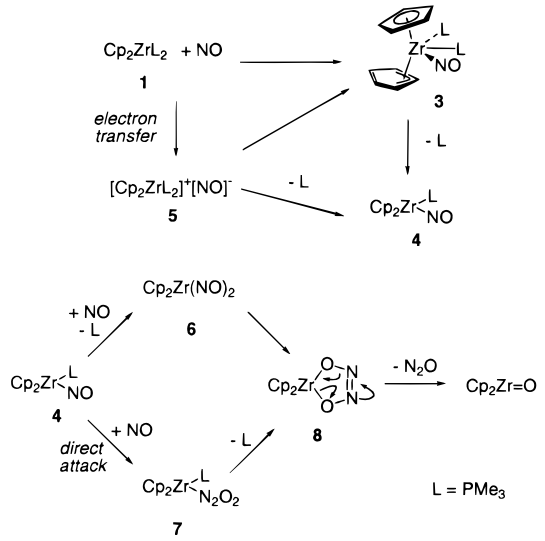

Mechanism of Reduction of NO by 1. On the basis of the above analysis, we conclude that nitric oxide is reduced to nitrous oxide by $Cp_2Zr(PMe_3)_2$ in a sequence of steps that are very fast and that occur near or at the gas−solvent interface. Our proposed mechanism is outlined in Scheme 4. The kinetics indicate a bimolecular reaction as the initial, rate-controlling process. This is possibly a bimolecular ligand substitution process similar to that observed by Basolo, Rausch, and coworkers in the PR_3-for-CO ligand substitution at $Cp_2Zr(CO)_2$. For this process, an η^3-Cp intermediate, $(\eta^3\text{-Cp})(\eta^5\text{-Cp})Zr(CO)_2(PR_3)$, was proposed.[46] An analogous ligand substitution process leading to $Cp_2Zr(PMe_3)(NO)$ (**4**) would have the intermediate structure $(\eta^3\text{-Cp})(\eta^5\text{-Cp})Zr(PMe_3)_2(NO)$ (**3**). However, the rate constant for the bimolecular reaction observed in this study is approximately 10^8 M^{-1} s^{-1}, which is 11 orders of magnitude faster than those observed by Basolo and Rausch. Alternatively, the rate-limiting bimolecular step may be an outer-sphere electron-transfer process, leading to ion pair **5**.[47] Ligand

(45) Barrow, G. M. *Physical Chemistry*, 5th ed.; McGraw-Hill: New York, 1988.

(46) Palmer, G. T.; Basolo, F.; Kool, L. B.; Rausch, M. D. *J. Am. Chem. Soc.* **1986**, *108*, 4417.

(47) We thank a reviewer for this suggestion.

substitution at the cationic Zr(III) center in **5** would be much faster than that at Zr(II) in **1**. While this would provide an explanation for the very fast bimolecular rate observed, further studies are required in order to rigorously establish the presence or absence of an electron-transfer pathway.

The subsequent steps in the transformation of NO to N_2O are even faster than the initial bimolecular process, and their exact nature is unclear. One reasonable product-forming intermediate is a zirconium dinitrosyl complex (**6**), since it is known that dinitrosylmetal complexes often decompose to give oxo species and N_2O.[38] The dinitrosyl complex **6** could arise from a second ligand substitution (NO for PMe_3). Alternatively, the second NO may attack the nitrosyl ligand directly, as has been proposed by Trogler and co-workers for the reduction of NO to N_2O by Pd^{2+} salts.[10] Such a process would produce an N−N-bonded species, $Cp_2Zr(PMe_3)(N_2O_2)$ (**7**). Each of these intermediates could lead to $Cp_2Zr(N_2O_2)$ (**8**), either through coupling of the nitrosyl ligands in complex **6** or through loss of a phosphine ligand from complex **7**. Complex **8** could then decompose to $Cp_2Zr{=}O$ and N_2O.

We favor a chelating hyponitrite structure for complex **8**, as shown in Scheme 4, based upon the chemistry of zirconium tetrazene complexes, the all-nitrogen analogues of a chelating hyponitrite complex (eq 21). The tetrazene complexes have been shown to cleave reversibly to give organic azides and imido complexes, the isoelectronic nitrogen analogues of $Cp_2Zr{=}O$ and nitrous oxide.[48]

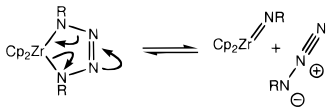

(21)

Conclusion

$Cp_2Zr(PMe_3)_2$ (**1**) reacts quickly with nitric oxide to produce nitrous oxide and $Cp_2Zr{=}O$. This reaction is so rapid that this chemical process is kinetically competitive with transport of NO into THF solution. The kinetic data were interpreted using the chemical absorption formalism outlined by Astarita,[44] in which penetration of the liquid surface by gaseous NO is important in the reaction kinetics. The data indicate that a bimolecular reaction between NO and **1** is the chemically rate-limiting step. The nitrous oxide produced is further reduced to dinitrogen by addition of an additional equivalent of **1**. In both of these reductions, the $Cp_2Zr{=}O$ produced may be trapped by either Cp_2ZrMe_2 or Me_3SiCl, prior to its oligomerization.

Experimental Section

General Methods. Unless otherwise indicated, all reactions were performed under an inert atmosphere (N_2, Ar, or He). A description of instrumentation and general procedures has been published.[48] Unless otherwise specified, all reagents were purchased from commercial suppliers and used without further purification. PMe_3 (Strem or Aldrich) was dried over Na prior to use. 2,5-Dimethyltetrahydrofuran (Aldrich, mixture of cis and trans) was dried first over CaH_2 and then over sodium/benzophenone ketyl. NO (Matheson) was purified by passage through two −130 °C traps. N_2O (Airco) was purified by passage through a −78 °C trap. In the trapping studies, control experiments were performed which verified that the traps did not react with the nitrogen oxide substrates under the relevant reaction conditions—Cp_2ZrMe_2 does not react with N_2O, and Me_3SiCl does not react with either N_2O or NO at room temperature in benzene or THF.

$Cp_2Zr(PMe_3)_2$ (1). The following synthesis is based on that published for other bis-phosphine complexes by Gell and Schwartz.[49] It was found to provide the product in higher purity than the published procedure.[50,51] PMe_3 (25 mL) was condensed into an evacuated flask containing $Cp_2Zr(H)(CH_2Cy)$[52] (Cy = cyclohexyl) (911 mg, 2.9 mmol), cooled to −196 °C. The reaction flask was warmed to 0 °C, and the contents were stirred for 2 h (until all of the $Cp_2Zr(H)(CH_2Cy)$ dissolved). The volatile materials were removed in vacuo, and the black-red residue was extracted with pentane (3 × 8 mL). The combined extracts were filtered through a column of Celite (2 cm × 1 cm), and the filtrate was evaporated to dryness in vacuo to yield a brown solid (690 mg, 1.9 mmol, 64%). ^{1}H NMR (400 MHz, C_6D_6, 20 °C): δ 4.81 (s, br), 0.99 (s, br). $^{31}P\{^1H\}$ NMR (162 MHz, C_6D_6, 20 °C): δ 18.9 (s, br). Lit.[50] ^{1}H NMR (90 MHz, toluene-d_8, −20 °C): δ 4.75 (t, J = 2.0 Hz, 10 H), 0.96 (vt, J = 4.9 Hz, 18 H). $^{31}P\{^1H\}$ NMR (toluene-d_8, −20 °C): δ 24.0.

Reaction of 1 with NO. Method A. NO (5.0 μmol) was transferred under vacuum into an NMR tube containing **1** (1.2 mg, 3.2 μmol) and p-$(MeO)_2C_6H_4$ (an internal standard, 1.4 mg, 10 μmol) in C_6D_6 (0.5 mL) at −196 °C. The tube was flame-sealed. Upon thawing of the solution, fast bleaching of the dark red color was observed along with precipitation of a colorless material. A yield of 21 ± 2% $[Cp_2ZrO]_3$ (δ 6.21) was calculated by integration of the product peak vs the internal standard.

Method B. A degassed solution of $Cp_2Zr(PMe_3)_2$ (181 mg, 0.485 mmol) in THF (10 mL) was cooled to −78 °C and exposed to NO (mmol) with stirring for 20 min. The gaseous materials were removed in vacuo, and the solution and precipitate were transferred to a centrifuge tube by cannula. Following centrifugation, the supernatant was removed, and the precipitate of $[Cp_xZrO_y]_n$ was washed with hexanes (3 × 10 mL).

Reaction of 1 with NO in the Presence of Me_3SiCl. NO (0.26 mmol) was transferred under vacuum into a glass bomb containing **1** (96 mg, 0.26 mmol) and Me_3SiCl (0.48 mmol) in C_6H_6 (15 mL) at −196 °C. Upon thawing of the solution, fast bleaching of the dark red color was observed. The volatile materials were removed in vacuo, leaving a pale yellow residue. The residue was extracted with toluene (3 × 8 mL), and the combined extracts were filtered through a short column of Celite (1 cm × 2 cm). The pale yellow filtrate was cooled to −35 °C overnight. Colorless crystals were recovered (20 mg, 22% yield). ^{1}H NMR (400 MHz, C_6D_6): δ 5.93 (s, 10 H), 0.11 (s, 9 H). $^{13}C\{^1H\}$ NMR (100 MHz, C_6D_6): δ 114.2, 1.9. Lit.[16] ^{1}H NMR: δ 6.00 (s, 10 H), 0.12 (s, 9 H). $^{13}C\{^1H\}$ NMR: δ 114.0, 1.8. The identity of the isolated material was further confirmed by comparison with an authentic sample of **2** prepared from Cp_2ZrCl_2 and $KOSiMe_3$.[17]

In a separate experiment, NO (7.1 mmol) was transferred under vacuum into an NMR tube containing **1** (2.3 mg, 6.2 mmol), Me_3SiCl (11 mmol), and p-$(MeO)_2C_6H_4$ (an internal standard, 1.1 mg, 8.0 mmol) in C_6D_6 (0.5 mL) at −196 °C. Fast reaction was apparent upon thawing of the solution. A yield of 77 ± 2% $Cp_2Zr(OSiMe_3)(Cl)$ was calculated by integration of the product peaks vs the internal standard.

Reaction of 1 with N_2O. A degassed, frozen solution (−78 °C) of $Cp_2Zr(PMe_3)_2$ (3.2 mg, 8.6 μmol) and p-$(MeO)_2C_6H_4$ (internal standard, 1.5 mg, 11 μmol) in C_6D_6 (0.5 mL) was exposed to N_2O (ca. 0.5 atm). The tube was flame-sealed and warmed to room temperature. Upon thawing of the solution, bleaching of the dark red color and deposition of a precipitate was observed. ^{1}H NMR spectroscopic analysis showed 26 ± 2% $[Cp_2ZrO]_3$ by integration of the product peak against the internal standard.

Reaction of 1 with N_2O in the Presence of Me_3SiCl. A stirred solution (−78 °C) of **1** (120 mg, 0.32 mmol) and Me_3SiCl (75 μL, 0.59 mmol) in C_6H_6 was exposed to N_2O (1 atm) for 10 min. The solution was brought to room temperature over 30 min. The volatile materials were removed in vacuo, and the pink residue was extracted with toluene (6 × 8 mL). The extracts were combined and the volatile

(48) Meyer, K. E.; Walsh, P. J.; Bergman, R. G. *J. Am. Chem. Soc.* **1995**, *117*, 974.

(49) Gell, K. I.; Schwartz, J. *J. Chem. Soc., Chem. Commun.* **1979**, 244.

(50) Kool, L. B.; Rausch, M. D.; Alt, H. G.; Herberhold, M.; Honold, B.; Thewalt, U. *J. Organomet. Chem.* **1987**, *320*, 37.

(51) Kool, L. B.; Rausch, M. D.; Alt, H. G.; Herberhold, M.; Thewalt, U.; Honold, B. *J. Organomet. Chem.* **1986**, *310*, 27.

(52) *KaleidaGraph*, version 3.06; Synergy Software, 1996.

materials removed. The faint pink residue was washed with cold toluene (2 × 5 mL). The washed material (now colorless) was dissolved in toluene (ca. 15 mL), filtered through Celite (1 cm × 2 cm column), and concentrated to ca. 5 mL. The toluene solution was cooled to −35 °C for 12 h. Colorless crystals of $Cp_2ZrCl(OSiMe_3)$ were recovered (43 mg, 39% yield). ^{1}H NMR (400 MHz, C_6D_6): δ 5.93 (s, 10 H), 0.11 (s, 9 H). $^{13}C\{^1H\}$ NMR (100 MHz, C_6D_6): δ 114.2, 1.9. Lit.[15] ^{1}H NMR: δ 6.00 (s, 10 H), 0.12 (s, 9 H). $^{13}C\{^1H\}$ NMR: δ 114.0, 1.8. The identity of the isolated material was further confirmed by comparison with an authentic sample of **2** prepared from Cp_2ZrCl_2 and $KOSiMe_3$.[17]

In a separate experiment, N_2O (18 μmol) was condensed into an NMR tube containing a degassed, frozen solution of **1** (3.0 mg, 8.0 μmol), Me_3SiCl (18 μmol), and *p*-$(MeO)_2C_6H_4$ (as an internal standard, 5.0 mg, 36 μmol) in toluene-d_8. Fast reaction was observed upon thawing of the solution. ^{1}H NMR spectroscopic analysis showed 102 ± 2% $Cp_2Zr(OSiMe_3)(Cl)$ by integration of the product peak against the internal standard.

Reaction of 1 with N_2O in the Presence of Cp_2ZrMe_2. N_2O (31 μmol) was condensed into an NMR tube containing a degassed, frozen solution (−78 °C) of $Cp_2Zr(PMe_3)_2$ (3.0 mg, 8.0 μmol), Cp_2ZrMe_2 (3.0 mg, 12 μmol), and *p*-$(MeO)_2C_6H_4$ (an internal standard, 3.0 mg, 22 μmol) in C_6D_6 (0.5 mL). The tube was sealed and warmed to room temperature. Upon thawing of the solution, bleaching of the dark red color was observed. ^{1}H NMR spectroscopic analysis showed 76 ± 2% $[Cp_2ZrMe]_2O$ by integration of the product peaks against the internal standard.

Gas Chromatography: General Procedures. Headspace gas analysis was performed using either a Varian Aerograph 90-P or 920 gas chromatograph. A CTR-I column (Alltech) comprised of two coaxial columns with different packings (hydrophobic polymer mixture/molecular sieves) was employed and was found to provide good separation of the gaseous analytes important to this study (N_2, O_2, NO, N_2O) at room temperature. Calibration experiments with known volumes showed that the GC response for each of these gases varied linearly with molar amount. The GC response was calibrated prior to use by injection of standard samples. To account for the different partitioning between the solvent and headspace for the various gases, standard curves relating the headspace concentration and the total amount of a given analyte were prepared for each solvent and temperature used.

Gas Chromatography: Reaction of 1 with NO. The gaseous products from the reaction of **1** with both a stoichiometric amount and a molar deficiency of NO were examined. The reaction apparatus and procedures were effectively identical in both cases. A vial (12.2 mL) equipped with a small stir bar was charged with 5.0 mL of a toluene solution of **1** (0.013 M, 65 μmol). The vial was sealed with a three-holed screw cap over a GC septum. The solution was degassed by bubbling He gas through it for ca. 2 min. The reaction vial was then fitted with two syringes: a 5.0-mL gastight syringe equipped with a stopcock charged with 3.0 mL of NO (130 μmol), and a 5-mL glass syringe filled with 1.3 mL of He. The second syringe provided a means of measuring the system volume. The barrel of this syringe was lubricated with mineral oil to allow smooth movement and to prevent leaking of gas in to or out of the reaction vial. The NO was added all at once. The system volume was observed to increase by ca. 3 mL (a reading of 4.3 mL on the volume-monitoring syringe) and then to decrease over 1 min to a net 1.4 mL increase (a reading of 2.7 mL). Analysis of the headspace gas by GC showed a N_2O/N_2 ratio of 5:1, and NO was not detected. Conversion of the headspace concentrations to total quantities of N_2O and N_2 gave 44 (68%) and 8.1 (12%) μmol, respectively. Based on the total volume of change observed, 107 ± 10% of the NO was consumed.

In the case where a deficiency of NO was employed, **1** (17.4 mg, 47 μmol) was treated with 0.52 mL of NO (23 μmol). Headspace gas analysis showed a N_2O/N_2 ratio of 1:20, and no NO was detected. Total quantities of N_2O and N_2 determined from the headspace concentrations were 0.8 ± 0.3 (7%) and 10 ± 0.3 (86%) μmol, respectively.

Control experiments in which no $Cp_2Zr(PMe_3)_2$ was added showed no consumption of NO and no N_2 from leaks.

Table 1. Gas Chromatographic Data for the Conversion of N_2O to N_2 by $Cp_2Zr(PMe_3)_2$

entry	N_2O injected (mL)	N_2 produced (mL)	yield (%)
1	0.50	0.33	66
2	1.00	0.94	94
3	1.50	1.32	88
4	2.00	1.64	82

Table 2. FTIR Data for the Conversion of NO to N_2O by $Cp_2Zr(PMe_3)_2$

	$Cp_2Zr(PMe_3)_2$ (**1**)		NO (μmol)		N_2O (μmol) produced (yield, %)
entry	mg	μmol	initial	remaining (yield, %)	
1	11.6	31.0	60.4	*b*	29.5 (98)[a]
2	14.2	38.1	72.9	*b*	33.8 (93)[a]
3	6.1	16	151	75.3 (79)[c]	33.5 (69)[c]
4	7.1	19	132	20.1 (98)[c]	49.3 (87)[c]

[a] Based upon stoichiometry of eq 2. [b] None detected. [c] Based upon stoichiometry of eq 6.

Gas Chromatography: Reaction of 1 with N_2O. A 50-mL Schlenk flask equipped with a stir bar was charged with a solution of **1** (63 mg, 170 μmol) in toluene (5.0 mL). The contents were degassed by three freeze−pump−thaw cycles, and 1 atm of He was placed over the solution. N_2O was added by syringe in four batches (0.50 mL, 22 μmol each). After each addition, the reaction mixture was allowed to stir for 10 min, and then the headspace gas was analyzed by GC. The results of these analyses are listed in Table 1. N_2 was produced in 86 ± 9% yield based on N_2O added.

Infrared Spectroscopy. A cylindrical cell (20 cm × 2 cm) with CaF_2 windows and a sidearm (4 cm × 1 cm) was employed in these experiments. In a typical procedure, the cell was evacuated, and NO (60.4 μmol) was transferred into the liquid nitrogen-cooled sidearm. Upon thawing of the solution, an initial spectrum of the NO was acquired. The NO in the cell was then condensed into an evacuated flask containing **1** (14.2 mg, 38.1 μmol) in toluene (15 mL). After the solution was stirred for 20 min at 20 °C, the volatile materials were transferred into the sidearm of the IR cell. Upon thawing of the solution, an infrared spectrum of the gas-phase materials was acquired. Comparison of the integrated infrared band intensities against standard curves gave quantitative values for the NO consumed (>58 μmol, >96%) and N_2O produced (29.5 ± 0.5 μmol, 98% yield). Data from these experiments are given in Table 2.

Kinetic Measurements: General Procedure. A schematic representation of the apparatus is shown in Figure 1. In a typical procedure, a three-necked flask was loaded with a solution of the reactants in the glovebox. The flask was also fitted with a known-volume bulb (6.6 mL). Outside the glovebox, one of the stoppers on the flask was replaced with an adapter, connecting the flask to a pressure transducer (Baratron) under flow of inert gas (Ar or N_2). The system was degassed by two freeze−pump−thaw cycles. The known-volume bulb was charged with NO (typically 100 Torr). After temperature equilibration, a pulse of NO was introduced by opening the stopcock separating the NO-containing bulb and the reaction flask. The pressure was recorded by charting the dc output from the pressure gauge using a chart recorder. Commercial software was used to fit data and calculate endpoints.[52]

The stirring rates for the stirring plate used (IKA, RCT basic) were determined in an experiment performed with Mr. Jake Yeston. A Teflon-coated stir bar, modified previously to have a hole halfway through the bar along the stirring axis, was mounted with epoxy to the Teflon tip of a syringe plunger, normally used with a gastight syringe. The tip of the syringe plunger, and thus the stir bar, could spin freely on the body of the plunger. The beam chopper of a flash photolysis apparatus, described elsewhere,[53] was removed and replaced with the modified stir bar suspended above the stir plate. The stir bar was placed such that it blocked the IR laser beam when the stir bar's long axis

(53) Schultz, R. H.; Bengali, A. A.; Tauber, M. J.; Weiller, B. H.; Wasserman, E. P.; Kyle, K. R.; Moore, C. B.; Bergman, R. G. *J. Am. Chem. Soc.* **1994**, *116*, 7369.

Table 3. Kinetic Data for the Reaction of NO with PMe_3 in THF (195 K) at 19.6 Hz Stir Rate

entry	[PMe_3] (M)	P_{NO} (init) (Torr)	n_{NO} (init) (μmol)	$k_{obs} \times 10^2$ (s^{-1})	$k \times 10^2$ (M^{-1} s^{-1})
1	1.07	18.7	110	1.45(6)	1.36(7)
2	1.05	12.8	75	1.56(4)	1.48(5)
3	1.03	2.4	14	1.22(2)	1.16(3)
4	1.03	2.0	12	1.20(2)	1.17(3)

Table 4. Kinetic Data for the Reaction of NO with PMe_3 in THF (195 K)

entry	[PMe_3] (M)	P_{NO} (init) (Torr)	n_{NO} (init) (μmol)	stir rate (Hz)	$k_{obs} \times 10^2$ (s^{-1})	$k \times 10^2$ (M^{-1} s^{-1})
1	0.84	5.2	31	21.7	1.35(3)	1.61(4)
2	0.83	5.2	31	19.6	1.28(2)	1.54(3)
3	0.83	5.2	31	15.7	1.19(2)	1.43(3)
4	0.82	5.2	31	11.8	1.14(2)	1.39(2)
5	0.82	5.2	31	9.35	1.06(2)	1.29(2)

was perpendicular to the beam but allowed the beam to pass to the detector when its long axis was parallel to the beam. In this way, the stir bar acted as a beam chopper, blocking the beam twice per revolution. The stirring rate was measured for stirring speeds important to this study (ca. 10−25 Hz) by reading the chop period from the oscilloscope.

Kinetic Measurements: Reaction of PMe_3 with NO. These reactions were run at −78 °C with an 11.0-mL solution of PMe_3 (1.1 M) in THF. The procedure followed is described in the general section above. In each experiment, first-order decay of the pressure was observed (Figure 2). The total volume of the system was determined to be 120 ± 4 mL. These values were used for calculation of the bimolecular rate constant according to the method of Kuhn et al. (eq 22), assuming a dimensionless Henry's constant, H, of 0.5 (V_g = volume of the gas, V_l = volume of the liquid).

$$k = \frac{k_{obs}(HV_g + V_l)}{[PMe_3]V_l} \qquad (22)$$

The bimolecular rate constant for the reaction of PMe_3 and NO (k_{PMe_3}) at this temperature was found to be $(1.3 \pm 0.1) \times 10^{-2}$ M^{-1} s^{-1}. Specific data for these reactions are given in Tables 3 and 4.

Kinetic Measurements: Reaction of 1 with NO. The apparatus and procedure were effectively identical to those used in the kinetic study of the reaction of PMe_3 with NO**,** except that the total solution volume was 10.0 mL. The conditions of each experiment are recorded in Tables 5 and 6. The zero-order and first-order regimes of each decay were easily deconvoluted by inspection of the pressure (P) vs time (t) and $\ln(P_f - P)$ vs t plots.

Some of the reactions were run at 160 K, which is below the freezing point of pure THF (164.8 K). The presence of solutes lowers the freezing point, and others have reported freezing points below 150 K for THF solutions in cryoscopy experiments.[54] The concentrations employed in this work give expected freezing point depressions between 3 and 6 K (depending on the value of the cryoscopy constant, K_f, used).[54,55] At 160 K, these solutions were fluid and nonviscous.

Acknowledgment. We thank Prof. Richard A. Andersen (Department of Chemistry, University of California, Berkeley) and Prof. Philip M. Gschwend (Department of Civil and Environmental Engineering, Massachusetts Institute of Technology) for helpful discussions and Prof. David L. Sedlak and Ms. Abra Bentley (Department of Civil and Environmental Engineering, University of California, Berkeley) for use of their gas chromatograph. This work was supported by NSF Grant No. CHE-9416833.

Table 5. Kinetic Data for the Reaction of NO and $Cp_2Zr(PMe_3)_2$ in THF at 19.6 Hz Stir Rate

entry	P_{NO} (init) (Torr)	n_{NO} (init) (μmol)	temp (K)	[**1**] (mM)	[PMe_3] (M)	J_{NO}[a] (μmol cm^{-2} s^{-1})	k_{obs}[b] (s^{-1})
1	8.23	48.3	160	102	0.88	1.72	0.78
2	6.30	36.9	160	91	0.88	1.56	1.06
3	6.30	36.9	160	87	0.88	1.44	0.89
4	6.30	36.9	160	84	0.88	1.57	1.17
5	6.12	35.9	160	79	0.00	1.02	0.48
6	6.78	39.8	160	70	0.00	1.71	0.57
7	1.21	7.1	178	28	1.00	0.69	0.74
8	1.82	10.7	178	85	0.24	1.87	1.50
9	2.06	12.1	178	84	0.48	1.67	1.52
10	2.54	14.9	178	82	0.96	2.71	1.30
11	6.66	39.1	178	66	0.00	2.72	1.05
12	5.15	30.2	195	29	1.00	1.44	0.61
13	3.57	21.0	195	32	0.00	1.45	0.80
14	3.57	21.0	195	30	0.00	1.16	0.79
15	3.57	21.0	195	27	0.01	1.19	0.59
16	3.39	19.9	195	11	0.00	0.55	0.63
17	3.39	19.9	195	9	0.01	0.39	0.40
18	1.15	6.7	195	6	0.00	0.26	0.42
19	0.97	5.7	195	4	0.00	0.17	0.25
20[c]	4.66	27.3	195	46	0.00	1.73	0.61
21[c]	5.81	34.1	195	43	0.00	1.71	0.51
22[c]	5.81	34.1	195	40	0.00	1.52	0.48

[a] Apparent zero-order flux from the beginning of each kinetic run. [b] Pseudo-first-order rate constant from the end of each kinetic run. [c] Reaction performed in 2,5-dimethyltetrahydrofuran.

Table 6. Kinetic Data for the Reaction of NO and $Cp_2Zr(PMe_3)_2$ in THF (195 K)

entry	P_{NO} (init) (Torr)	n_{NO} (init) (μmol)	stir rate (Hz)	[**1**] (mM)	J_{NO}[a] (μmol cm^{-2} s^{-1})	$k_L°$ (cm s^{-1})
1	1.88	11.0	21.7	14	1.43	0.31
2	5.52	32.3	21.7	32	2.73	0.26
3	1.88	11.0	19.6	12	0.78	0.20
4	4.85	28.4	19.6	35	2.69	0.23
5	1.88	11.0	15.7	9.6	0.43	0.14
6	1.88	11.0	11.8	7.4	0.19	0.079
7	5.14	30.1	11.8	29	0.92	0.097
8	1.88	11.0	9.4	5.2	0.099	0.058

[a] Apparent zero-order flux from the beginning of each kinetic run.

Table 7. Calculated Values for the Viscosity of THF, the Diffusivities of NO and **1**, and the Diffusion-Controlled Rate Constant at Various Temperatures

		$D \times 10^6$ (cm^2 s^{-1})		
T (K)	η(THF) (cP)	NO	**1**	$k_{diff} \times 10^{-9}$ (M^{-1} s^{-1})
160	6.2	3.3	0.50	1.7
178	3.5	6.5	0.99	3.4
195	2.3	11	1.7	5.8
298	0.47	83	13	43

Appendix

A.1. Viscosity. The viscosity of THF was calculated using eq 23, which gives values in units of Pa/s. To convert to cP (mPa/s), one must multiply by 10^3. The equation and constants were obtained from Daubert et al.[56] For temperatures where a comparison is available, the calculated viscosities (Table 7)

(54) Gerold, A.; Jastrzebski, J. T. B. H.; Kronenburg, C. M. P.; Krause, N.; van Koten, G. *Angew. Chem., Int. Ed. Engl.* **1997**, *36*, 755.

(55) Cooper, A. R. *Determination of Molecular Weight*; John Wiley and Sons: New York, 1989; Vol. 103.

(56) Daubert, T. E.; Danner, R. P.; Sibul, H. M.; Stebbins, C. C. *Physical and Thermodynamic Properties of Pure Chemicals: Data Compilation*; Taylor & Francis: Washington, DC, 1997.

agree very well with published values determined by experiment.[57]

$$\eta = \exp\left(-1.03 + \frac{884}{T} - 5.27 \ln T\right) \quad (23)$$

A.2. Diffusivity. The diffusivity of NO in THF was calculated using the method of Wilke and Chang[58] (eq 24), where Φ is the solvent association factor, M_{solv} is the molecular weight of the solvent in g mol^{-1}, T is the temperature in K, η is the viscosity of the solvent in cP, and V_{solute} is the molecular volume of NO in cm^3 mol^{-1}. An association factor of $\Phi = 1$ was used,

$$D = \frac{7.4 \times 10^{-8}(\Phi M_{solv})^{0.5} T}{\eta_{solv}(V_{solute})^{0.6}} \quad (24)$$

and the molecular volume of NO was taken to be 13.9 cm^3 mol^{-1}.[56] The diffusivity of **1** was calculated similarly using a molecular volume of 324 cm^3 mol^{-1}. This molecular volume was arrived at by calculating the volume of the Cp and phosphine ligands by the group contribution method of Fuller et al.[59] and adding the spherical volume of the Zr atom (r = 1.06 Å).[60] The calculated diffusivities are given in Table 7. At all temperatures, the ratio $D_{NO}/D_{\mathbf{1}}$ is 6.6.

Using the diffusivities, the diffusion-controlled rate constant can be estimated according to eq 25.[43,45] In this expression, r is the spherical radius, and N_A is Avogadro's number. Calculated values of k_{diff} using r_{NO} = 1 Å and $r_{\mathbf{1}}$ = 5 Å are presented in Table 7.

$$k_{diff} = 4\pi(D_{NO} + D_{\mathbf{1}})(r_{NO} + r_{\mathbf{1}})N_A \quad (25)$$

A.3. Interfacial Surface Area. The interfacial surface area (A) is a crucial component in the calculation of the flux of nitric oxide into solution. Unfortunately, the rapid stirring employed in the experiments makes it difficult to know the surface area accurately. Our estimate is based on the mathematical description of the stirred solution vortex by Nagata.[61] It assumes a smooth, well-defined surface and does not take into account irregularities such as ripples and momentary splashes. Accordingly, *this estimate should be viewed as a lower limit.* The vortex shape can be described by a parabola within a certain radius and by a hyperbola outside of it. The cross section of our model interfacial surface is shown in Figure 8. The interior portion (radius < 1 cm) of the cross section is described by $z = kx^2 - k$, and the exterior portion (1 cm < radius < 2 cm) is described by $z = k - kx^{-2}$, where k is half the depth of the vortex. For our calculations, k = 1 cm. The surface of revolution generated by rotation of this cross section about the bisecting axis has a surface area of 9.4 cm^2.

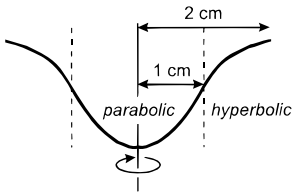

Figure 8. Cross section of the model interfacial surface.

A.4. Henry's Law Constant. Since no data were available for the solubility of NO in THF (dielectric constant, ϵ = 18.5), this value for H was estimated to be 0.5 from the Henry's constants for EtOAc (ϵ = 6.02, H_{195} = 0.84) and CH_3CN (ϵ = 35.0, H_{195} = 0.34).[62,63] While this method of estimation is crude, it is supported by the fact that the solubility of NO is similar ($0.35 < H_{195} < 1.1$) for the range of organic solvents reported (e.g., hexanes, toluene, Et_2O, CCl_4), and it is relatively insensitive to temperature.[62,63]

JA983011P

(57) Carvajal, C.; Toelle, K. J.; Smid, J.; Szwarc, M. *J. Am. Chem. Soc.* **1965**, *87*, 5548.
(58) Reid, R. C.; Prausnitz, J. M.; Poling, B. E. *The Properties of Gases and Liquids*, 4th ed.; McGraw-Hill: New York, 1987.
(59) Fuller, E. N.; Schettler, P. D.; Giddings, J. C. *Ind. Eng. Chem.* **1966**, *58*, 19.
(60) *CRC Handbook of Chemistry and Physics*, 72nd ed.; Lide, D. R., Ed.; CRC Press: Boca Raton, FL, 1991.
(61) Nagata, S. *Mixing: Principles and Applications*; Kodansha Ltd.: Tokyo, 1975.
(62) Fogg, P. G. T.; Gerrard, W. *Solubility of Gases In Liquids*; John Wiley and Sons Ltd.: Chichester, UK, 1991.
(63) *Oxides of Nitrogen*; Young, C. L., Ed.; Pergamon Press: Oxford, 1981; Vol. 8, pp 160−349.